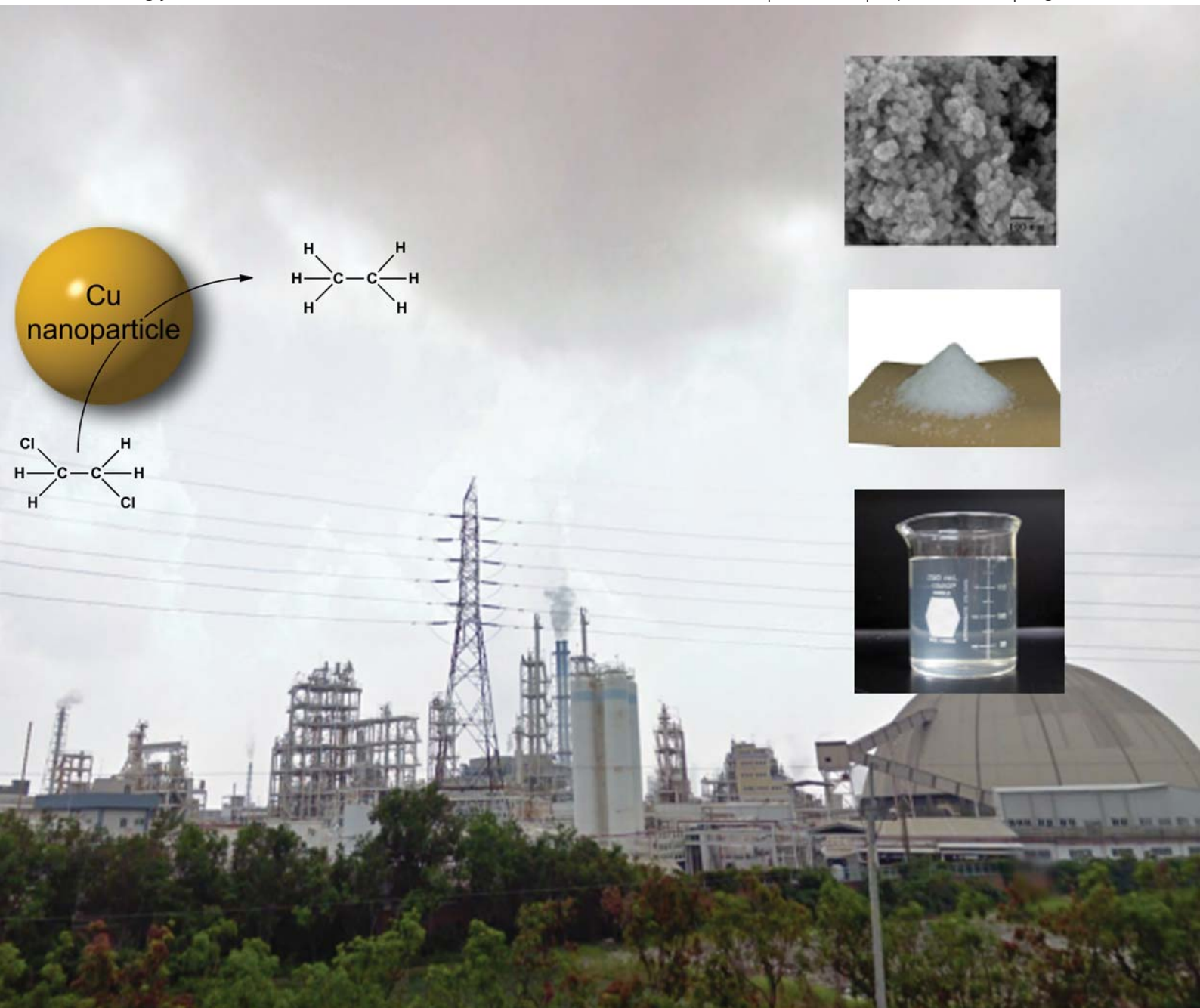


# Journal of Environmental Monitoring

Cutting-Edge Research on Environmental Processes & Impacts

www.rsc.org/jem

Volume 13 | Number 9 | September 2011 | Pages 2337–2660



ISSN 1464-0325

RSC Publishing

**PAPER**

Lien *et al.*

Catalytic hydrodechlorination of 1,2-dichloroethane using copper nanoparticles under reduction conditions of sodium borohydride

## Catalytic hydrodechlorination of 1,2-dichloroethane using copper nanoparticles under reduction conditions of sodium borohydride

Chang-Chieh Huang,<sup>a</sup> Shang-Lien Lo,<sup>a</sup> Shin-Mu Tsai<sup>b</sup> and Hsing-Lung Lien<sup>\*b</sup>

Received 1st May 2011, Accepted 22nd July 2011

DOI: 10.1039/c1em10370a

1,2-Dichloroethane (1,2-DCA) is a raw material used for the manufacture of vinyl chloride monomer (VCM) and therefore has very often been detected in the groundwater nearby the VCM manufacturing plant. Zero-valent iron (ZVI) is capable of degrading a wide array of highly chlorinated contaminants; however, the reactivity of ZVI towards 1,2-DCA is very low. In this study, zero-valent copper nanoparticles have been synthesized for effective dechlorination of 1,2-DCA under reduction conditions of sodium borohydride. Copper nanoparticles consisted of mainly metallic copper (Cu<sup>0</sup>) with small amounts of cuprous oxide (Cu<sub>2</sub>O). They have surface areas of about 19.0 m<sup>2</sup> g<sup>-1</sup> and an average diameter of 15 nm. Batch experiments were conducted to test the effectiveness of copper nanoparticles for 1,2-DCA degradation using sodium borohydride as electron donors where the ORP was measured as -1100 mV. More than 80% of 1,2-DCA (30 mg L<sup>-1</sup>) was rapidly degraded within 2 h in the presence of both copper nanoparticles (2.5 g L<sup>-1</sup>) and borohydride (25 mM). No reduction of 1,2-DCA was observed when the system contained either copper nanoparticles alone or borohydride alone. The degradation intermediates included ethane and ethylene accounting for 79% and ~1.5% of the 1,2-DCA lost, respectively. Potential environmental applications can be achieved by immobilizing copper nanoparticles onto the surface of reducing metals to form a reactive bimetallic structure.

### Introduction

1,2-Dichloroethane (1,2-DCA) is one of the chlorinated aliphatic hydrocarbons frequently found in surface and groundwater sources. It is used in vinyl chloride monomer (VCM) and polyvinyl chloride (PVC) manufacturing processes.<sup>1</sup> Because of improper handling, storage or disposal practices, a widespread contamination of groundwater by 1,2-DCA has been reported. For example, 1,2-DCA was detected in 17% of groundwater samples obtained from 479 waste disposal sites in the United

States.<sup>2</sup> Recently, a PVC manufacturing facility in Taiwan has been identified as the likely source of groundwater contaminated by 1,2-DCA at a concentration of 15 100 mg L<sup>-1</sup>, more than 300 000 times higher than the corresponding groundwater quality standard established by the Taiwanese Environmental Protection Administration.<sup>3</sup> Because 1,2-DCA causes circulatory and respiratory failure associated with neurological disorders in human beings<sup>4</sup> and is a suspected carcinogen, there is a need to develop effective technologies for remediation of 1,2-DCA.

Chemical reduction is a classical method applied to many remedial technologies such as zero-valent iron (ZVI) and nano-sized ZVI (NZVI) for the degradation of chlorinated organic contaminants.<sup>5-9</sup> Not surprisingly, the reduction of chlorinated aliphatic hydrocarbons in the presence of electron donors is thermodynamically favourable under ambient conditions. For

<sup>a</sup>Graduate Institute of Environmental Engineering, National Taiwan University, Taipei, 106, Taiwan

<sup>b</sup>Department of Civil and Environmental Engineering, National University of Kaohsiung, Kaohsiung, 811, Taiwan. E-mail: lien.sam@nuk.edu.tw; Fax: +886-7591-9376; Tel: +886-7591-9221

### Environmental impact

1,2-Dichloroethane (1,2-DCA) is a raw material used for the manufacture of vinyl chloride monomer (VCM) and therefore has very often been detected in the groundwater nearby the VCM manufacturing plant. Although nano-sized and micro-sized zero-valent iron (ZVI) are capable of degrading a wide array of highly chlorinated contaminants *e.g.*, trichloroethylene; the reactivity of ZVI towards 1,2-DCA is very low. We report here a novel material, zero-valent copper nanoparticle, for the effective dechlorination of 1,2-DCA under reducing conditions. To the best of our knowledge, copper nanoparticles are the only zero-valent metal possessing the ability to degrade 1,2-DCA under reducing conditions. Potential environmental applications can be achieved by immobilizing copper nanoparticles onto the surface of reducing metals to form a reactive bimetallic structure.

example, ZVI has been demonstrated capable of treating highly chlorinated aliphatic hydrocarbons containing either one or two carbon atoms.<sup>10,11</sup> The use of NZVI tends to increase the degradation rate of chlorinated organics by 1–2 orders of magnitude, compared with commercial ZVI.<sup>9</sup> Currently, an increasing number of field remediation has been implemented using NZVI as the reactive reagent for the removal of chlorinated organic solvents in groundwater.<sup>12–16</sup>

Regardless of the capability of remediating a variety of chlorinated organics, it has been found that the reactivity of either ZVI or NZVI towards 1,2-DCA is very low.<sup>10,17,18</sup> Studies using different zero-valent metals (*e.g.*, Zn) or bimetals (*e.g.*, Pd/Fe) to degrade 1,2-DCA also showed the reaction is slow.<sup>18,19</sup> Liu *et al.* have reported the use of the electrolytic reduction of chlorinated aliphatic compounds to investigate the relationship between reaction rates and characteristics of target compounds including C–Cl bond dissociation energies (or C–Cl bond strengths) and standard reduction potentials.<sup>20</sup> They concluded that log-transformed reaction rate constants for reduction of chlorinated alkanes were linearly related to C–Cl bond strengths where increasing in bond strengths decreased reaction rates. The lack of reactivity towards 1,2-DCA may therefore be attributed to the relatively high C–Cl bond strength compared to the higher chlorinated ethanes. For example, the bond strength of hexachloroethane and 1,1,1-trichloroethane was 68.83 and 73.6 kcal mol<sup>-1</sup>, respectively, whereas the reaction rate of hexachloroethane was four times higher than that of 1,1,1-trichloroethane in reaction with palladized NZVI under identical conditions.<sup>20</sup>

Thus, a catalyst capable of weakening the C–Cl bond strength should enhance the degradation rate of 1,2-DCA. Many catalysts including Pd–Ni, Pt–Sn and Pt–Cu have been reported for effective hydrodechlorination of 1,2-DCA; however, they were applied to gaseous 1,2-DCA at relatively high temperature conditions (>100 °C).<sup>21–23</sup> In the aqueous phase, group VIII metal-based catalysts such as palladium and platinum are effective for hydrodechlorination of chlorinated organics with the number of chlorine substituents equal to or greater than three in the presence of hydrogen but are generally less effective for hydrodechlorination of less chlorinated organics such as 1,2-DCA and dichloromethane. On the other hand, group IB metal-based catalysts such as copper are less effective than group VIII metal-based catalysts for hydrodechlorination but are able to degrade less chlorinated organics such as dichloromethane.<sup>22</sup>

In this study, we present the use of copper nanoparticles for effective degradation of 1,2-DCA under reducing conditions. Copper is known as a mild hydrogenation catalyst.<sup>24</sup> It is effective for most of the elementary reactions that are required in catalytic dehalogenation.<sup>25</sup> Resin-supported zero-valent copper nanoparticles with the size of 10 nm in diameter have been documented to have the surface area normalized rate constant ( $k_{SA}$ ) 110–120 times higher than copper powder for the dechlorination of carbon tetrachloride.<sup>26</sup> However, because copper itself with a standard reduction potential of +0.34 V possesses a very low reducing power, the use of external reducing reagents is needed to facilitate the reduction reaction. Borohydride has been known as a strong reductant and a hydrogen storage material.<sup>27</sup> Hydrogen gas is readily generated through the hydrolysis of sodium borohydride with water. Accordingly,

sodium borohydride was selected in the study. The objectives of this study included to synthesize the copper nanoparticles, to examine the reaction rate and analyze the product distribution, and to investigate the dose effect of electron donors and copper nanoparticles on the effectiveness of 1,2-DCA degradation.

## Experimental methods

### Chemicals and materials

Reagent grade 1,2-DCA (99.8%), sodium borohydride (NaBH<sub>4</sub>, 99%) and poly(acrylic acid), sodium salt (PAA) powder with a typical molecular weight of 2100 g mol<sup>-1</sup> were purchased from Sigma-Aldrich. *n*-Hexane (99%) was obtained from Riedel-deHaën. Cupric sulfate pentahydrate (CuSO<sub>4</sub>·5H<sub>2</sub>O, 99.5%) was obtained from Yakuri Pure Chemicals Co. Ltd. Analytical standard of 1,1-dichloroethane (1,1-DCA; 5000 µg mL<sup>-1</sup> in methanol, ampule of 1 mL) and a standard gas mixture for GC analysis containing 1% each of ethane, ethylene, acetylene, and methane were purchased from Supelco. Copper powder (99+%) and palladium 1 wt% on alumina were obtained from Lancaster and Sigma-Aldrich, respectively.

### Synthesis of copper nanoparticles

The borohydride reduction has widely been used for the preparation of nanoparticles such as iron and copper nanoparticles.<sup>8,13,28,29</sup> In this work, the synthesis of copper nanoparticles was achieved by adding a 1 : 1 volume ratio of NaBH<sub>4</sub> (0.13 M) into CuSO<sub>4</sub> (0.04 M). The solution was mixed vigorously at room temperature for 1 min (22 ± 1 °C). The synthesized metal particles were then washed with a large volume (1000 mL) of Milli-Q water at least three times. Dispersion of copper nanoparticles was conducted by using PAA as a stabilizer. PAA stabilized copper nanoparticles were prepared by the same procedures as described above except for mixing PAA with the NaBH<sub>4</sub> solution. The dose of PAA accounted for 10% by weight of the mass of copper nanoparticles. It should be noted that PAA stabilized copper nanoparticles were only used in morphological analysis with TEM and zeta potential analysis.

### Batch experiments

Batch tests were conducted in 165 mL glass vials containing 30 mg L<sup>-1</sup> of 1,2-DCA in a 100 mL aqueous solution. Prior to the reaction, each vial was loaded with various amounts of copper nanoparticles and sodium borohydride as a catalyst and reductant, respectively. Batch bottles were mixed on an orbital shaker (175 rpm) at room temperature (22 ± 1 °C). The batch vials were periodically sampled by transferring sample aliquots (0.5 mL) into 2 mL of *n*-hexane. The extraction was performed for 30 min on the orbital shaker (175 rpm).

### Analytical methods

Analysis of dichloroethanes was conducted by a solvent extraction method. A 2.5 µL extract was withdrawn for GC analysis where the split ratio was set at 4. The GC (HP 6890) was equipped with an electron capture detector and a DB-5 capillary column (J&W, 30 m × 0.53 mm). Temperature conditions for

oven, injection port, and detector were set at 50, 200 and 300 °C, respectively. Concentrations of hydrocarbons were measured by a HP4890 GC equipped with a flame ionization detector and a HP-PLOT/Q capillary column (J&W, 30 m × 0.53 mm). A 50 µL headspace gas aliquot was withdrawn by a gastight syringe for GC analysis. The same temperature program as described above was used for the hydrocarbon analysis except that the oven temperature was set at 40 °C. Concentrations of 1,2-DCA, 1,1-DCA and hydrocarbons were determined by the external standard method using calibration curves. Calibration curves for each compound were made initially and the variability was checked daily before analysis (<15%). Analysis was generally performed in triplicate with relative differences less than 15%.

Chloride concentrations were analyzed on a Metrohm 861 Advanced Compact ion chromatograph equipped with a Metrosep A Supp 5-100/4.0 column. An eluent containing 9 mM Na<sub>2</sub>CO<sub>3</sub>/2.8 mM NaHCO<sub>3</sub> was used. The eluent flow was set at 0.7 mL min<sup>-1</sup>. The experiments were conducted in triplicate.

Measurements of the oxidation–reduction potential (ORP) and pH were carried out by an Orion pH/mV meter equipped with a combination redox electrode and a combination pH electrode. The redox electrode uses a 4 M KCl reference solution saturated with AgCl. Thus, the measured ORP values are converted to the redox potential ( $E_h$ ) values by adding 200 mV to the ORP voltage.

### Solid phase characterization

Morphological and elemental analyses of copper nanoparticles were performed by a scanning electron microscope (SEM) (Hitachi S-4300, Hitachi Science Systems, Ltd.) equipped with an energy-dispersive X-ray (EDX) spectroscope at 10 kV and a field emission transmission electron microscope (TEM) (Hitachi Model HF-2000) at 120 kV. X-Ray diffraction (XRD) measurements were conducted to characterize the surface composition of copper nanoparticles using an X-ray diffractometer (Siemens D5000) with a copper target tube radiation (Cu K<sub>α</sub>) producing an X-ray with a wavelength of 1.54056 Å. Samples were placed on a quartz plate and were scanned from 20 to 80° (2θ) at a rate of 5° 2θ (1/min). A surface area analyzer (Beckman Coulter SA3100) was used to determine surface areas of copper nanoparticles. The zeta potential of copper nanoparticles in aqueous solutions was measured by a zeta potential analyzer (ZetaPlus, Brookhaven Instruments Corporation). The solid loading was 0.2 g L<sup>-1</sup> in a 10<sup>-2</sup> M NaCl aqueous solution.

## Results and discussion

### Characterization of copper nanoparticles

Fig. 1 depicts SEM and TEM images of copper nanoparticles. The SEM image, taken in the absence of stabilizers, shows the copper nanoparticles agglomerate (Fig. 1a). The aggregation of nanoparticles is a natural tendency in the absence of stabilizers.<sup>8,30</sup> On the other hand, well-suspended copper nanoparticles with an average diameter on the order of 10–15 nm were observed in the presence of PAA (Fig. 1b). PAA is a commonly used stabilizer for nanoparticles. Other stabilizers such as oleylamine, triphenylphosphine, natural proteins, and dendrimers have also been used to disperse copper nanoparticles.<sup>8,28,29</sup>

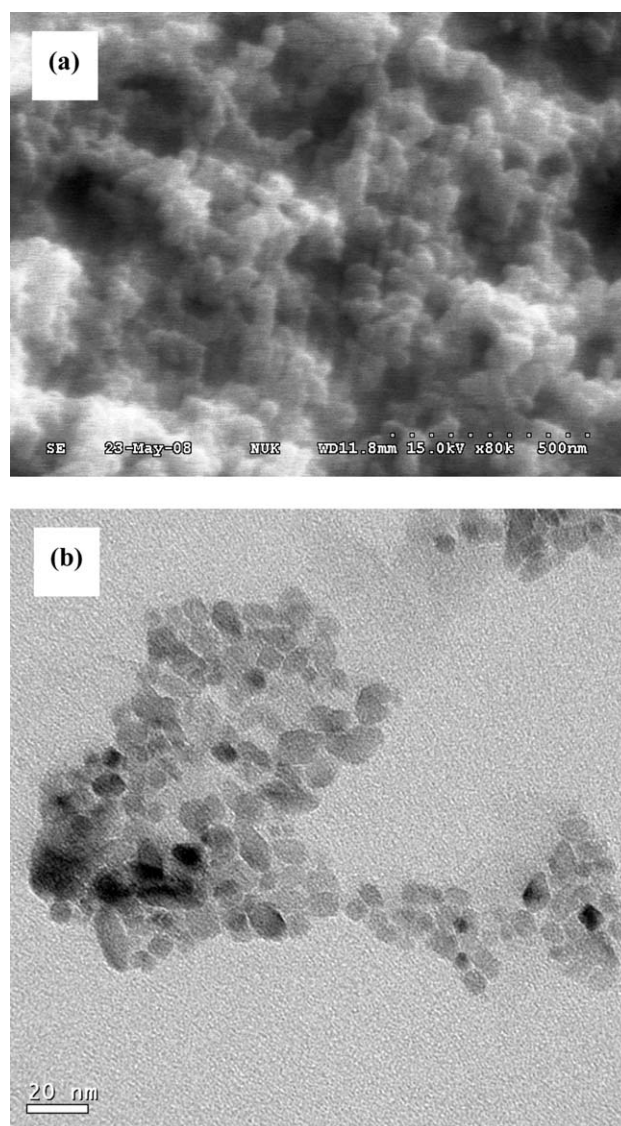


**Fig. 1** (a) A SEM image of copper nanoparticles prepared in the absence of stabilizers (80 000×) and (b) a TEM image of PAA-stabilized copper nanoparticles (100 000×).

The composition of copper nanoparticles was analyzed by SEM-EDX and XRD. Fig. 2a shows the EDX spectrum of typical copper nanoparticles indicating that copper was the major species accounting for 96% of the mass of nanoparticles. XRD analysis confirmed that the nanoparticles consisted of mainly metallic copper (Cu<sup>0</sup>) with small amounts of cuprous oxide (Cu<sub>2</sub>O) (Fig. 2b). The characteristic peaks of copper metal appeared at 43.316, 50.448, and 74.125° (2θ) (JCPDS 89-2838) and the peaks assigned to cuprous oxide were at the positions of 36.418, 42.297, 61.344, and 73.526° (2θ) (JCPDS 05-0667). According to the XRD analysis, cuprous oxide was observed to further reduce to copper within 24 h under borohydride reduction conditions as it was found the decrease in the cuprous oxide peak of 36.418° and the increase in the copper peaks of 43.316 and 50.448° (Fig. 2b). This is consistent with the fact that cuprous oxide is a partial oxidation product of metallic copper.

BET surface analysis indicated that the specific surface area of copper nanoparticles was in an average of 19 ± 1.1 m<sup>2</sup> g<sup>-1</sup>, which

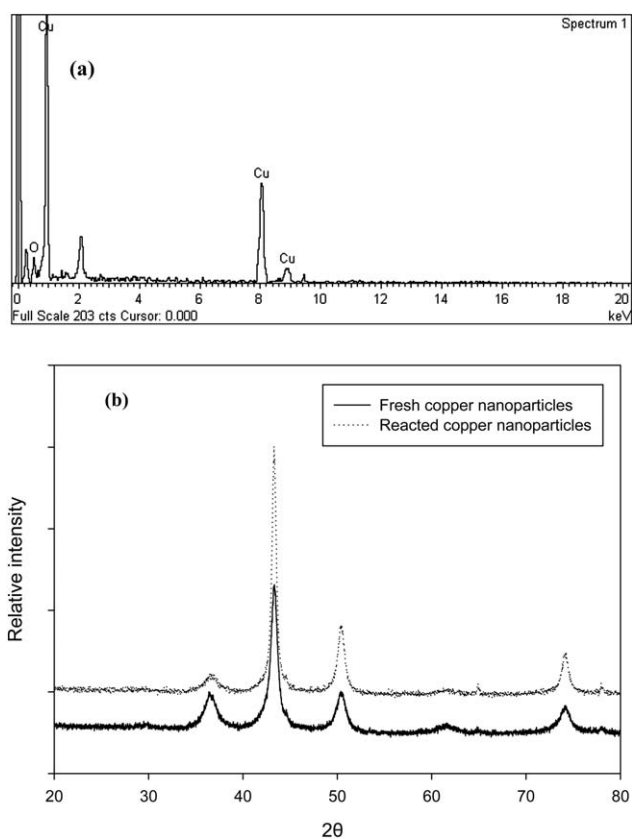


**Fig. 2** (a) SEM-EDX spectrum of copper nanoparticles and (b) XRD spectra of copper nanoparticles before and after reaction with 1,2-DCA under reducing conditions.

is relatively smaller than that of NZVI particles.<sup>8,9</sup> The zero point of charge ( $\text{pH}_{\text{zpc}}$ ) for copper nanoparticles was determined to be at  $\text{pH}$  9.2 (Fig. 3). This reveals that copper nanoparticles are positively charged under near neutral  $\text{pH}$  conditions. Because aquifer materials are usually negatively charged, copper nanoparticles with a positively charged surface at a  $\text{pH}$  below 9.2 would be unfavourable to transport in groundwater. It should be

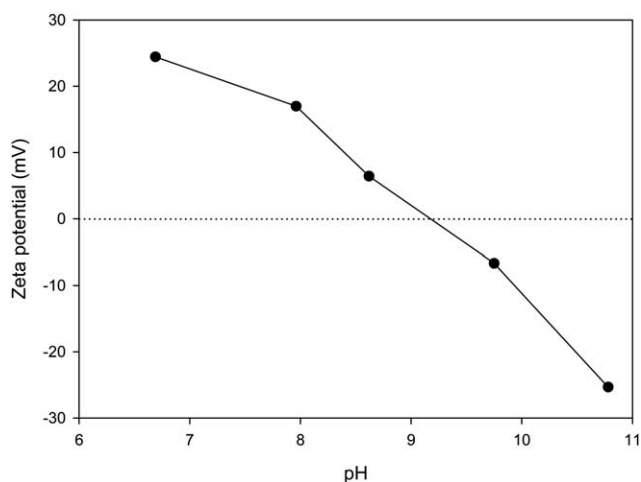


**Fig. 3** Effects of  $\text{pH}$  on the zeta potential of PAA stabilized copper nanoparticles.

pointed out effects of  $\text{pH}$  on the zeta potential of copper nanoparticles varied from surfactant to surfactant. For example, copper nanoparticles stabilized with hexadecyl trimethyl ammonium bromide (CTAB) exhibited only a positive charge of zeta potential while those stabilized with sodium dodecylbenzenesulfonate (SDBS) showed only a positive charge of zeta potential in the  $\text{pH}$  range of 2 to 12.<sup>31</sup>

### Degradation of 1,2-DCA

Degradation of 1,2-DCA using copper nanoparticles under borohydride reduction conditions is shown in Fig. 4. Approximately 85% of 1,2-DCA was rapidly reduced within 5 h. No further reduction of 1,2-DCA was found after 5 h. Control tests indicated that 1,2-DCA cannot be reduced either in the presence of copper nanoparticles alone or under borohydride reduction conditions alone. Nevertheless, it is worth pointing out that 1,1-DCA is readily reduced under borohydride reduction conditions without copper nanoparticles. The disappearance of 1,1-DCA accounted for about 62% of initial 1,1-DCA concentrations within 10 h in the presence of borohydride alone. 1,2-DCA is more resistant than 1,1-DCA to be dechlorinated under reduction conditions of sodium borohydride. Among many factors (*e.g.*, chemical structure and degree of chlorination) influencing the reactivity of a specific chlorinated compound, the bond strength should be taken into consideration for surface-mediated reactions. The bond strength of the C–Cl bond for 1,2- and 1,1-DCA is 82.23 and 79.12  $\text{kcal mol}^{-1}$ , respectively,<sup>20</sup> suggesting that 1,2-DCA is more recalcitrant than 1,1-DCA for the reduction, which is consistent with this study.

Furthermore, as shown in Fig. 4, palladium/alumina is unable to catalytically dechlorinate 1,2-DCA under borohydride reduction conditions. Besides the direct reduction occurring at the metal surface, palladium has been known as an effective catalyst for hydrodechlorination through the indirect reduction

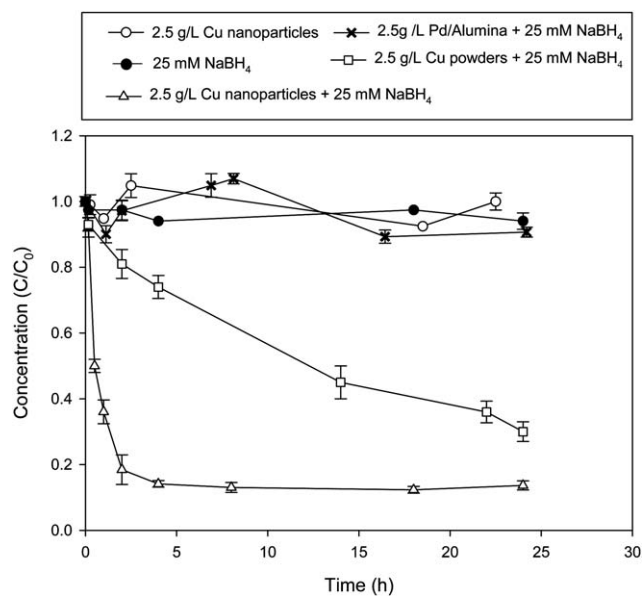
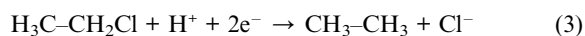
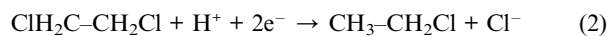


**Fig. 4** Degradation of 1,2-DCA ( $30 \text{ mg L}^{-1}$ ) by copper nanoparticles, micro-sized copper particles and palladium/alumina under reducing conditions (25 mM  $\text{NaBH}_4$ ).

involving the formation of atomic hydrogen as a very powerful reducing reagent to reductively dechlorinate contaminants.<sup>9,32</sup> In this study, hydrogen evolution occurred *via* the hydrolysis of sodium borohydride in reaction with water accomplishing a favourable condition to the indirect reduction with palladium. However, no reduction of 1,2-DCA in the presence of palladium indicated that the reductive dechlorination of 1,2-DCA did not undergo indirect reduction.

Degradation of 1,2-DCA takes place *via* two different reaction pathways under reducing conditions.<sup>33</sup> 1,2-DCA is transformed in a single step *via* reductive dihaloelimination to ethylene (eqn (1)) while in two consecutive hydrogenolysis reactions yielding chloroethane (eqn (2)) and ethane (eqn (3)).



In this study, the product analysis revealed that ethane was the major product accounting for 79% of the 1,2-DCA lost while the yield of ethylene was only 1.1%. The carbon mass balance was determined to be about 70% of the initial 1,2-DCA concentration, consistent with the chlorine mass balance measured by the IC analysis. The product analysis suggested that 1,2-DCA underwent two consecutive hydrogenolysis reactions with copper nanoparticles. Ethylene was detected in a trace amount suggesting that dihaloelimination was a minor reaction pathway. However, it should be noticed that the possibility of dihaloelimination of 1,2-DCA to ethylene that further undergoes hydrogenation to ethane cannot be ruled out. A further investigation of chloroethane production is needed.

### Dosage effects of electron donors and copper nanoparticles

Effects of the reductant concentration on the effectiveness of 1,2-DCA degradation are illustrated in Fig. 5. As shown in Fig. 5, an increase in the concentration of borohydride tends to increase the degradation effectiveness of 1,2-DCA in the presence

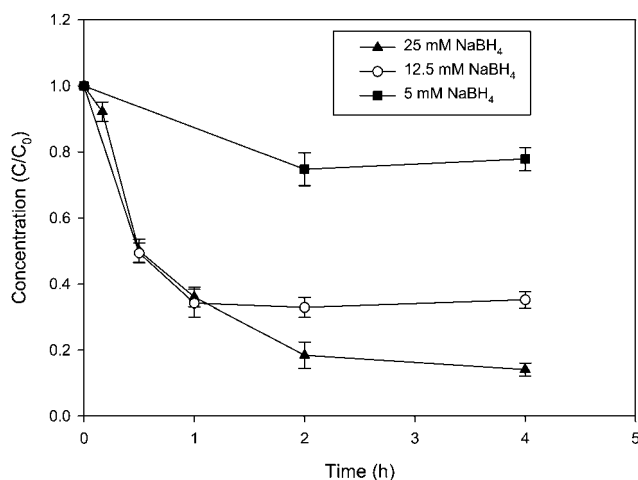


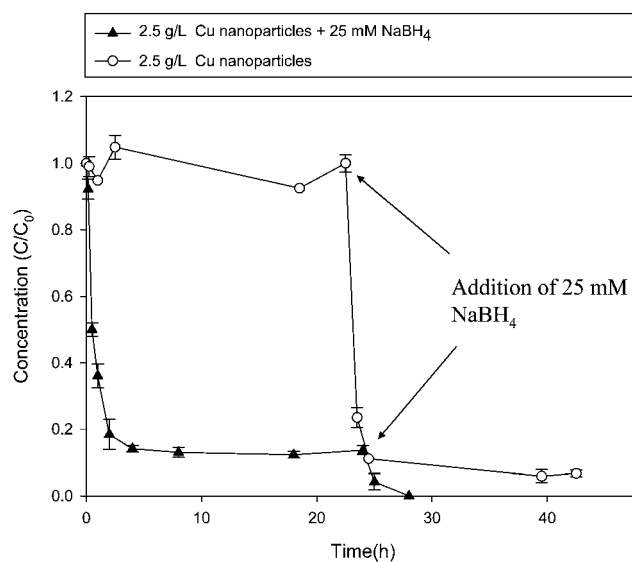
**Fig. 5** Effects of sodium borohydride concentrations on 1,2-DCA degradation with 2.5 g L<sup>-1</sup> copper nanoparticles.

of the same metal loading (2.5 g L<sup>-1</sup> of copper nanoparticles). At the low borohydride concentration (5 mM), about 20% of the initial 1,2-DCA was degraded while the degradation efficiency increased to 85% of the total amount of 1,2-DCA at the borohydride concentration of 25 mM. Measurements of ORP revealed more negative values of ORP were detected with increasing borohydride concentrations implying more strongly reducing conditions occurred at higher borohydride concentrations. The ORP values decreased from -22, -600, to -1100 mV as borohydride concentrations increased from 0, 12.5, to 25 mM, respectively, suggesting that the 1,2-DCA degradation rate is a function of the reducing power.

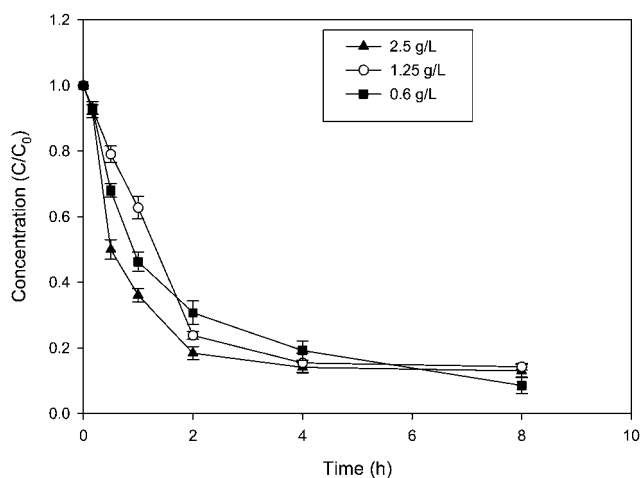
The significance of the reductant was further confirmed by repetitive experiments with the addition of sodium borohydride. Fig. 6 shows that no reduction of 1,2-DCA was found in the presence of copper nanoparticles alone for 24 h while a rapid reduction occurred after the addition of sodium borohydride. Similar results were also observed in the presence of both copper nanoparticles and reductant where the efficiency of the 1,2-DCA degradation was increased from 80% to nearly 100% after sodium borohydride was added at 24 h. This suggested that no further reduction of 1,2-DCA after 5 h shown in Fig. 4 is resulted from the decrease of the reducing power provided by sodium borohydride.

Fig. 7 illustrates the metal dose effect of copper nanoparticles on the 1,2-DCA degradation rate under identical reduction conditions (25 mM NaBH<sub>4</sub>). Unlike the effect of the reductant, the metal dose of copper nanoparticles exhibited a similar effect on the 1,2-DCA degradation rate. In the previous literature, a pseudo-first-order kinetics model has been most frequently used to describe the reaction rate of the metal-mediated degradation.<sup>10</sup> For 1,2-DCA, the equation can be expressed as follows:

$$\frac{dC}{dt} = -k_{\text{obs}}C \quad (4)$$



**Fig. 6** The addition of sodium borohydride (25 mM NaBH<sub>4</sub>) into the 1,2-DCA reaction system containing copper nanoparticles (2.5 g L<sup>-1</sup>) after 24 h.



**Fig. 7** Effects of copper nanoparticle dose on the 1,2-DCA degradation rate under reducing conditions (25 mM NaBH<sub>4</sub>).

where  $C$  is the concentration of 1,2-DCA ( $\text{mg L}^{-1}$ );  $k_{\text{obs}}$  is the observed rate constant ( $\text{h}^{-1}$ ) and  $t$  is the time ( $\text{h}$ ). The observed first-order rate constants of the 1,2-DCA reduction for the metal dose of 2.5, 1.25 and  $0.6 \text{ g L}^{-1}$  were therefore determined to be 0.49, 0.49 and  $0.40 \text{ (1/h)}$ , respectively. In contrast, the 1,2-DCA reduction by micro-sized copper powders was observed at a significantly slow rate. The observed first-order rate constant was calculated to be about  $0.046 \text{ (1/h)}$ , 10 times lower than that of copper nanoparticles. This can be attributed to the large difference at the surface area for these two types of copper particles. The specific surface area of copper nanoparticles was about  $19 \text{ m}^2 \text{ g}^{-1}$ , which is almost 65 times larger than that of micro-sized copper powder ( $0.29 \text{ m}^2 \text{ g}^{-1}$ ). Because the surface area determines the intrinsic reactivity of the surface-mediated reaction, when taken into account, the reaction rate constant can be expressed as surface area normalized rate constants:<sup>10</sup>

$$k_{\text{obs}} = k_{\text{SA}} \rho a_s \quad (5)$$

where  $k_{\text{SA}}$  is the rate constant normalized to the specific surface area concentration ( $\text{L m}^{-2} \text{ per h}$ ),  $\rho$  is the metal concentration of copper ( $\text{g L}^{-1}$ ), and  $a_s$  is the specific surface area of copper ( $\text{m}^2 \text{ g}^{-1}$ ). As a result, the surface area normalized rate constant of copper nanoparticles at the metal dose of 2.5, 1.25, and  $0.6 \text{ g L}^{-1}$  was 0.010, 0.021, and  $0.035 \text{ L m}^{-2} \text{ h}^{-1}$ , respectively. Increasing the metal dose resulted in the decrease of the surface area normalized rate constant. For micro-sized copper powders, the  $k_{\text{SA}}$  value even increased to  $0.063 \text{ L m}^2 \text{ h}^{-1}$ . The inconsistency of  $k_{\text{SA}}$  between nano-sized and micro-sized particles is no surprise as Nurmi *et al.* have reported that iron nanoparticles may not be more reactive than micro-sized iron particles on a surface area normalized basis for carbon tetrachloride reduction.<sup>34</sup> Elliott *et al.* observed similar results in the study of dechlorination of hexachlorocyclohexanes and lindane with iron nanoparticles.<sup>35,36</sup> They noted that the specific surface area of nanoparticles tends not to be a static value over time but can vary as aggregation occurs. In this study, the inconsistency of  $k_{\text{SA}}$  values may also relate to an overdose of copper nanoparticles. Excessive amounts of copper nanoparticles aggregated and settled at the bottom of the reactor without reacting with 1,2-DCA.

## Potential application of copper nanoparticles

Because borohydride is expensive, the combination of copper nanoparticles with borohydride for 1,2-DCA degradation is not cost-effective. Further, the direct dispersion of copper nanoparticles either in the groundwater or wastewater treatment system is unaccepted because of the difficulty in recovering nanoparticles. The dissolution of copper nanoparticles may also cause concern on copper ion contamination. Though the USEPA has made a determination not to regulate boron with a national primary drinking water regulation,<sup>37</sup> no recommendation was made to directly use borohydride for groundwater remediation.

Immobilization of copper nanoparticles offers an opportunity for applying this nano-material to the environmental remediation. Immobilized copper nanoparticles can be achieved by dispersing copper nanoparticles onto a matrix.<sup>25</sup> The use of a reducing metal as a matrix impregnated with copper to form a so-called bimetallic structure may be applicable because the reducing metal can substitute borohydride to serve as electron donors. As shown in Fig. 5, the effective degradation of 1,2-DCA with copper nanoparticles required the ORP of  $-1100 \text{ mV}$ , which corresponds to the  $E_{\text{h}}$  of  $-900 \text{ mV}$ . At the higher ORP ( $> -600 \text{ mV}$ , or  $E_{\text{h}} > -400 \text{ mV}$ ), the reduction efficiency was significantly declined. This suggested that the reduction potential of reducing metals should be lower than  $-0.8 \text{ V}$ . Among many reducing metals applied in the reduction of chlorinated organics such as iron, zinc and aluminium,<sup>7,19,38,39</sup> aluminium with the standard reduction potential of  $-1.66 \text{ V}$  serves as a reactive reductant. Impregnation of aluminium with copper to form copper coated aluminium bimetallic particles has been developed.<sup>40</sup> Our studies have indicated that the bimetallic particles exhibited their ability for the dechlorination of dichloromethane, another recalcitrant contaminant unable to be degraded by NZVI in groundwater.<sup>40</sup> The dissolution of aluminium to soluble aluminium ions is a minor reaction for aluminium-based bimetals because an insoluble form of polymeric aluminium hydroxide dominates in reducing regions.<sup>41</sup> For example, concentrations of aluminium ions in the aqueous solution containing iron coated aluminium bimetals were measured to be about  $0.04 \text{ mg L}^{-1}$  at  $70 \text{ h}$ .<sup>39</sup>

## Conclusions

1,2-DCA is a very recalcitrant groundwater contaminant unable to be remediated by ZVI or NZVI. In this work, we demonstrated that copper nanoparticles can effectively degrade 1,2-DCA under reduction conditions of sodium borohydride. Based on the results of the study, the following conclusions can be drawn:

- Copper nanoparticles have a particle size on the order of 10–15 nm and an average surface area of  $19 \pm 1.1 \text{ m}^2 \text{ g}^{-1}$ . Copper nanoparticles consisted of mainly metallic copper ( $\text{Cu}^0$ ) with small amounts of cuprous oxide ( $\text{Cu}_2\text{O}$ ).
- Ethane was the major product during the 1,2-DCA degradation accounting for 79% of the 1,2-DCA lost. This suggests that 1,2-DCA undergoes two consecutive hydrogenolysis reactions with copper nanoparticles. Ethylene was detected in a trace amount ( $\sim 1\%$ ) suggesting that dihaloelimination is a minor reaction pathway. Yet, a further investigation of chloroethane production is needed to confirm the reaction pathways.

• The 1,2-DCA degradation rate is a function of reductant concentrations whereas an increase in the dosage of copper nanoparticles does not result in a corresponding increase in 1,2-DCA degradation rates. The latter may be attributed to the agglomeration and sedimentation of copper nanoparticles that reduce the available surface for the degradation of 1,2-DCA.

• Immobilization of copper nanoparticles onto the surface of reducing metals to form a bimetallic structure offers an opportunity for remediation applications because the reducing metal can substitute borohydride to serve as electron donors.

## Acknowledgements

The authors would like to thank National Science Council (NSC), Taiwan, ROC, for the financial support through NSC Grants (NSC 95-2221-E-390-014-MY2 and 96-2815-C-390-017-E).

## References

- 1 W. F. Carroll, T. C. Berger, F. E. Borrelli, P. J. Garrity, R. A. Jacobs, J. W. Lewis, R. L. McCreedy, D. R. Tuhovak and A. F. Weston, *Chemosphere*, 1998, **37**, 1957–1972.
- 2 G. C. Barbee, *Ground Water Monit. Rem.*, 1994, **14**, 129–140.
- 3 *Environmental Protection Administration, Taiwan, News Release (in Chinese)*, [http://ivy5.epa.gov.tw/enews/fact\\_HotFile.asp?inputtime=0990707173950](http://ivy5.epa.gov.tw/enews/fact_HotFile.asp?inputtime=0990707173950).
- 4 International Agency for Research on Cancer (IARC), in *Monographs on the Evaluation of the Carcinogenic Risk of Chemicals to Humans. Re-evaluation of Some Organic Chemicals, Hydrazine and Hydrogen Peroxide (Part Two)*, 1999, pp. 501–529.
- 5 R. W. Gillham and S. F. O'Hannesin, *Ground Water*, 1994, **32**, 958–967.
- 6 L. J. Matheson and P. G. Tratnyek, *Environ. Sci. Technol.*, 1994, **28**, 2045–2053.
- 7 T. J. Campbell, D. R. Burris, A. L. Roberts and J. R. Wells, *Environ. Toxicol. Chem.*, 1997, **16**, 625–630.
- 8 P. Jiemvarangkul, H. L. Lien and W. X. Zhang, *Chem. Eng. J.*, 2011, **170**, 482–491.
- 9 H. L. Lien and W. X. Zhang, *Appl. Catal., B*, 2007, **77**, 110–116.
- 10 T. L. Johnson, M. M. Scherer and P. G. Tratnyek, *Environ. Sci. Technol.*, 1996, **30**, 2634–2640.
- 11 A. L. Roberts, L. A. Totten, W. A. Arnold, D. R. Burris and T. J. Campbell, *Environ. Sci. Technol.*, 1996, **30**, 2654–2659.
- 12 United States Environmental Protection Agency (USEPA), *Nanotechnology for Site Remediation Fact Sheet*, 2008.
- 13 Q. L. Zhang, Z. M. Yang, B. J. Ding, X. Z. Lan and Y. J. Guo, *Trans. Nonferrous Met. Soc. China*, 2010, **20**, S240–S244.
- 14 Y. T. Wei, S. C. Wu, C. M. Chou, C. H. Che, S. M. Tsai and H. L. Lien, *Water Res.*, 2010, **44**, 131–140.
- 15 F. He, D. Y. Zhao and C. Paul, *Water Res.*, 2010, **44**, 2360–2370.
- 16 J. Quinn, C. Geiger, C. Clausen, K. Brooks, C. Coon, S. O'Hara, T. Krug, D. Major, W. S. Yoon, A. Gavaskar and T. Holdsworth, *Environ. Sci. Technol.*, 2005, **39**, 1309–1318.
- 17 R. Lookman, L. Bastiaens, B. Borremans, M. Maesen, J. Gemoets and L. Diels, *J. Contam. Hydrol.*, 2004, **74**, 133–144.
- 18 H. L. Lien and W. X. Zhang, *J. Environ. Eng.*, 2005, **131**, 4–10.
- 19 W. A. Arnold, W. P. Ball and A. L. Roberts, *J. Contam. Hydrol.*, 1999, **40**, 183–200.
- 20 Z. Liu, E. A. Betterton and R. G. Arnold, *Environ. Sci. Technol.*, 2000, **34**, 804–811.
- 21 D. R. Luebke, L. S. Vadlamannati, V. I. Kovalchuk and J. L. d'Itri, *Appl. Catal., B*, 2002, **35**, 211–217.
- 22 H. Xie, J. Y. Howe, V. Schwartz, J. R. Monnier, C. T. Williams and H. J. Ploehn, *J. Catal.*, 2008, **259**, 111–122.
- 23 A. Srebrowata, W. Juszczak, Z. Kaszkur and Z. Karpinski, *Catal. Today*, 2007, **124**, 28–35.
- 24 C. N. Satterfield, *Heterogeneous Catalysis in Industrial Practice*, McGraw-Hill, Inc., New York, NY, 2nd edn, 1991.
- 25 M. X. Yang, S. Sarkar, B. E. Bent, S. R. Bare and M. T. Holbrook, *Langmuir*, 1997, **13**, 229–242.
- 26 Y. H. Liou, S. L. Lo and C. J. Lin, *Water Res.*, 2007, **41**, 1705–1712.
- 27 S. S. Muir and X. Yao, *Int. J. Hydrogen Energy*, 2011, **36**, 5983–5997.
- 28 L. Balogh and D. A. Tomalia, *J. Am. Chem. Soc.*, 1998, **120**, 7355–7356.
- 29 M. J. Guajardo-Pacheco, J. E. Morales-Sanchez, J. Gonzalez-Hernandez and F. Ruiz, *Mater. Lett.*, 2010, **64**, 1361–1364.
- 30 W. Stumm and J. J. Morgan, *Chemical Equilibria and Rates in Natural Waters*, John Wiley & Sons, Inc, New York, 3rd edn, 1996.
- 31 X. Li, D. Zhu and X. Wang, *J. Colloid Interface Sci.*, 2007, **310**, 456–463.
- 32 T. Li and J. Farrell, *Environ. Sci. Technol.*, 2000, **34**, 173–179.
- 33 T. M. Vogel, C. S. Criddle and P. L. Mccarty, *Environ. Sci. Technol.*, 1987, **21**, 722–736.
- 34 J. T. Nurmi, P. G. Tratnyek, V. Sarathy, D. R. Baer, J. E. Amonette, K. Pecher, C. Wang, J. C. Linehan, D. W. Matson, R. L. Penn and M. D. Driessen, *Environ. Sci. Technol.*, 2004, **39**, 1221–1230.
- 35 D. W. Elliott, H. L. Lien and W. X. Zhang, *J. Environ. Eng.*, 2009, **135**, 317–324.
- 36 D. W. Elliott, H. L. Lien and W. X. Zhang, *J. Environ. Qual.*, 2008, **37**, 2192–2201.
- 37 United States Environmental Protection Agency (USEPA), *Regulatory Determinations Support Document for Selected Contaminants from the Second Drinking Water Contaminant Candidate List (CCL 2)*, EPA Report 815-R-08-012, 2008.
- 38 W. A. Arnold and A. L. Roberts, *Environ. Sci. Technol.*, 1998, **32**, 3017–3025.
- 39 L. H. Chen, C. C. Huang and H. L. Lien, *Chemosphere*, 2008, **73**, 692–697.
- 40 H. L. Lien and W. X. Zhang, *Chemosphere*, 2002, **49**, 371–378.
- 41 E. Deltombe and M. Pourbaix, *Corrosion*, 1958, **14**, 496–500.